JOURNAL OF PROPULSION AND POWER
Vol. 20, No. 5, September–October 2004

Simulation and Prediction of Magnetic Propellant Reorientation in Reduced Gravity

Jeffrey G. Marchetta* and John I. Hochstein†
University of Memphis, Memphis, Tennessee 38152-3180

Recent advances in magnet technology suggest that magnetic positive positioning of liquids may become a viable technology for future spacecraft systems. Development of a computational tool for simulation of this process is presented, as are results from experimental and computational studies. Simulation results that extend beyond the parameter space of the experimental investigation are presented to better understand this process and aid in the design of future experiments. A magnetic bond number is defined and serves as a valuable predictive correlating parameter for the investigation of magnetically induced propellant reorientation. Simulation predictions are presented and compared by the use of the magnetic bond number to determine if tank geometry, magnetic field configuration, tank fill, initial position, and *g* level have significant effects on the reorientation process. The influence of the magnetic field on propellant reorientation timing is also evaluated. Evidence is presented and conclusions are drawn that support the use of the simulation and the magnetic bond number as viable modeling and predictive tools in the continuing study of magnetic fluid positioning.

Nomenclature

$\hat{\boldsymbol{e}}_r, \hat{\boldsymbol{e}}_t$	=	unit vectors
f	=	volume of fluid function
g	=	acceleration due to gravity
H	=	magnitude of magnetic intensity
$\boldsymbol{H}$	=	magnetic intensity
L	=	characteristic length
$\boldsymbol{M}$	=	magnetization
m	=	magnetic dipole strength
n	=	coordinate normal to an interface
p	=	pressure
R	=	distance from dipole
r, y	=	radial and axial cylindrical coordinate directions
r, θ, ϕ	=	spherical coordinate subscripts
t	=	time
u, v	=	velocity in r and y directions
$\boldsymbol{V}$	=	velocity
κ	=	local surface curvature
μ	=	dynamic viscosity
μ_0	=	permeability of free space
ν	=	kinematic viscosity
ρ	=	density
σ	=	surface tension coefficient
χ	=	magnetic susceptibility
∇	=	nabla or del-operator

Introduction

RESEARCH and development of technologies, including analytical,[1] experimental,[2] and computational[3] studies, related to the management of cryogenic propellant systems in reduced-gravity environments, have yielded two general approaches to positive positioning. The first category includes passive systems, often referred to as liquid acquisition devices. This technology relies on capillary effects in special geometries within a tank to retain liquid within carefully shaped channels or traps.[4,5] These systems are currently used for the positioning of propellants used for satellite stationkeeping. Whereas such systems are adequate for certain applications, they add complexity and weight to the propellant tank. Also, their reliability for long-duration storage of cryogenic propellants is uncertain. The second category includes active systems that rely on impulsive settling or reorientation. Impulsive settling is accomplished by the firing of small auxiliary thrusters that accelerate the vehicle in a direction selected to move the liquid to the desired position within the tank.[3,6] This technology will reliably reorient liquid within a tank, even after extremely long dormant periods of spacecraft operation, provided that the acceleration level is adequate to overcome any retentive surface tension forces. Certain penalties accompany such systems, including the extra mass of propellant required for the auxiliary thrusters and the imposition of a required maneuver on the mission profile. An alternative concept, magnetic positive positioning, may evolve into a competitive third category and is the subject of the research reported herein.

The feasibility of the use of electromagnetic fields for liquid positioning in a reduced-gravity environment was explored in the early 1960s. However, the early studies[7] concluded that the use of electric fields for positive liquid positioning was an unacceptable safety risk because the potential existed of arcing within the tank due to a nonuniform distribution of electric charge. Another promising concept emerged that involved the use of magnetic fields and relied on the natural magnetic properties of the fluids. LO_2 is paramagnetic, or attracted to regions of high magnetic field strength, and LH_2 is weakly diamagnetic, or repelled from regions of high field strength. However, the magnetic forces are so weak that massive magnets would have been required to have a significant influence on liquid position within a full-scale tank. It was, therefore, concluded that this technology was impractical for use in a spacecraft propellant management system.

Recent successes with high-temperature superconducting materials have renewed interest in magnet positive positioning. A series of experiments to study magnetically actuated propellant orientation (MAPO)[8] were recently conducted. The objective of the program was to determine the feasibility of the use of a magnetic field to reorient liquid propellant positively within a tank and to maintain its position during propellant expulsion and tank filling operations. The experiments were performed with dilute ferrofluid/water mixture.

Presented as Paper 99-0845 at the AIAA 37th Aerospace Sciences Meeting and Exhibit, Reno, NV, 11–14 January 1999; received 5 December 2002; accepted for publication 24 September 2003.

*Assistant Professor, Department of Mechanical Engineering, 312 Engineering Sciences Building; jmarchtt@memphis.edu. Member AIAA.

†Professor, University of Memphis, Department of Mechanical Engineering, 312 Engineering Sciences Building. Associate Fellow AIAA.

A video camera recorded the liquid motion within a 10-cm-diam cylindrical transparent acrylic tank during the reduced gravity phase of the parabolic flight of the KC-135 aircraft. The flight provided only 20–30 s in which to conduct the experiment, and the flows were frequently influenced by unrepeatable initial conditions. Furthermore, the ferrofluid/water mixture only roughly approximates the physical properties of LO_2. Experimentation with LO_2 as the working fluid would increase by orders of magnitude the cost and complexity of the research program.

A purely experimental approach, encumbered by expense and time constraints, limits the ability to collect sufficient data for evaluation of the feasibility of magnetic positive positioning (MPP) for cryogenic propellant management. In addition, the complexity of the nonlinear physics associated with this technology makes development of a realistic analytic model unlikely. Therefore, a computational simulation is an attractive alternative for assessment of the feasibility of MPP of propellants for future spacecraft.

This paper presents results obtained by the use of a computational simulation specifically developed to emulate the motion of fluids under the influence of an imposed magnetic field in a reduced-gravity environment. Simulation flowfield predictions and flight images from the MAPO experiment were compared, and the validity of the use of the computational tool for modeling MPP was substantiated. Flow predictions and analyses that extended beyond the scope of MAPO experiment were conducted and evaluated with respect to a correlating parameter, the magnetic Bond number Bo_m. A minimum value of the magnetic bond number necessary to induce reorientation was sought for varying fill levels. These threshold values were then used to assess the utility of Bo_m as a dimensionless parameter for the prediction of reorientation in future experiments. Furthermore, a study of Bo_m predictions obtained from simulation results revealed the influence of varying gravity, tank shape, and fill level on settling time.

Mathematical Formulation

At the temperatures and pressures associated with cryogenic propellant storage tanks, LO_2 and LH_2 are well represented as incompressible, constant property, nonconducting, Newtonian fluids. Neuringer and Rosensweig[9] present a development of the momentum equation that describes the unsteady flow of such a fluid, culminating in the following modified Navier–Stokes equation.

$$\rho\frac{\partial \boldsymbol{V}}{\partial t} + \rho(\boldsymbol{V}\cdot\nabla)\boldsymbol{V} = -\nabla p + \mu\nabla^2\boldsymbol{V} + \rho\boldsymbol{g} + \boldsymbol{F}_M \tag{1}$$

where $\boldsymbol{F}_M = \mu_0(\boldsymbol{M}\cdot\nabla\boldsymbol{H})$.

For the flow of cryogenic propellants, it is appropriate to further assume that the magnetization is linear, that the magnetization is in the direction of the local magnetic field, and that the fluid susceptibility is constant. These assumptions permit simplification of the magnetic force term:

$$\boldsymbol{F}_M = \mu_0\chi H\nabla H \tag{2}$$

In the absence of significant temperature gradients, the tangential stress at a liquid/gas interface is typically negligible, and the normal stress at the interface is typically modeled as a pressure jump:

$$\Delta p = p - p_0 = \sigma\kappa - 2\mu\frac{\partial v_n}{\partial n} \tag{3}$$

For most applications, the viscous term is negligible compared to the surface tension term. Because the gas and liquid can have different magnetic susceptibilities, magnetic field lines may be bent at a gas/liquid interface, producing a normal stress at the interface. The resulting normal stress is frequently called the magnetic pressure and results in the following modified form of the normal stress boundary condition:

$$\Delta p = \sigma\kappa + \tfrac{1}{2}\mu_0\left[(\boldsymbol{M}\cdot\hat{n})^2_{\text{liq}} - (\boldsymbol{M}\cdot\hat{n})^2_{\text{gas}}\right] \tag{4}$$

For MPP, the magnetization of the liquid will be weak, and magnetization of the vapor will be negligible. Therefore, the magnetic pressure has been neglected and only the surface tension contribution to the normal stress at the interface is imposed in the computational model.

For the present study, a superconducting electromagnet positioned at the bottom of the tank is modeled as a magnetic dipole located on the tank centerline below the bottom of the tank. If the fluid magnetization is linear, the magnetic intensity field associated with the dipole is

$$\boldsymbol{H} = [1/(1+\chi)](m/4\pi R^3)[(2\cos\theta)\hat{\boldsymbol{e}}_r + (\sin\theta)\hat{\boldsymbol{e}}_\theta] \tag{5}$$

The product of the magnetic intensity gradient with its magnitude is used to compute the magnetic force.

The bond number represents the ratio of gravitational to surface tension forces and is frequently useful for the study of flows in a reduced-gravity environment:

$$Bo = \rho\ell^2 g/\sigma \tag{6}$$

By analogy, a dimensionless parameter formed by the ratio of the magnetic force to the surface tension force should be useful for the study of the MPP process. In Eq. (6), ρg is the magnitude of the gravitational force per unit volume in the direction of the gravity vector. A similar quantity to describe the paramagnetic force can be obtained by movement of the component of the magnetic force term of Eq. (2) in the direction of the desired reorientation. Thus, the magnetic bond number used for the present study has been defined as

$$Bo_m = (\ell^2/\sigma)\mu_o\chi_m|H\nabla H| \tag{7}$$

If $|H\nabla H|$ is constant over the entire field, a single value for Bo_m can be computed directly. However, if $|H\nabla H|$ is not constant, some averaging procedure is required if a single value for Bo_m is to be used for reorietation prediction.

Computational Model and Setup

A computational simulation was enhanced to simulate MPP.[10] The ability of this code and its variants[10] to model flows with highly deforming free surfaces in which surface tension forces are significant has been well documented,[10–13] as has their fidelity in modeling of the propellant reorientation process.[3,6] The unsteady, incompressible Navier–Stokes equations are discretized by the use of a staggered grid formulation, and the geometry is subdivided into finite volumes that form an Eulerian mesh. The solution to the resulting equations is advanced through time via a two-step projection method. The first step solves the momentum equations for initial estimates of the velocity components. A semi-implicit formulation, that uses an incomplete Choleski conjugate gradient iteration procedure, is solved to ensure that continuity is satisfied at every time step. This procedure is repeated for each time step, resulting in a simulation of unsteady flow.

The location of fluid within the mesh is determined by the use of the volume-of-fluid function f. The function is assigned a value of unity at a location occupied by fluid or a value of zero if there is no fluid present at that location. Partially filled cells are recognized by fractional values of f and the free surface location is the locus of points for which $f = \frac{1}{2}$. Surface tension forces are computed by the use of the continuum surface force model.[10]

To simulate magnetic positive positioning, the magnetic force was added to the representation of the momentum equation in the simulation, and several modifications to the input and output systems were made to support the magnetic model. The modified code is capable of representing a variety of magnetic fields and currently contains several cases for which the gradient of the field strength can be computed analytically. The code permits specification of the magnetic field based on measured data and is designed to interpolate the measured field onto a structured grid of unevenly spaced points. An analytical representation of the magnetic field for a dipole magnet model has also been included. The magnetic field can be

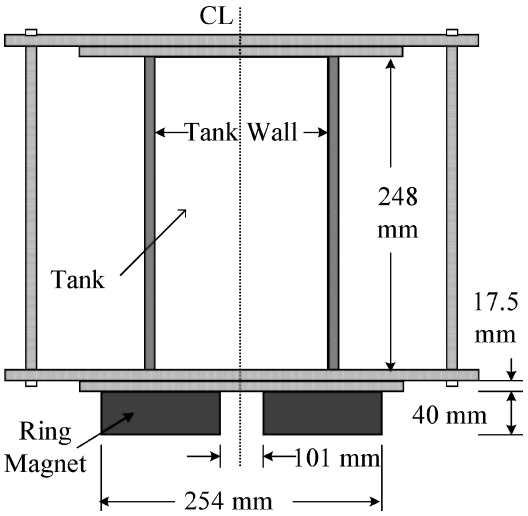

Fig. 1 MAPO experiment apparatus.

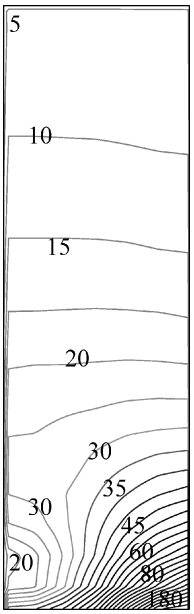

Fig. 2 Contours of constant magnetic intensity, H($\times 10^3$ A/m), inside the MAPO tank for the ring magnet.

determined by specification of a desired dipole strength or magnetic bond number in the input data. Further enhancement of code input includes variables for the designation of magnetic material properties.

Hochstein et al.[14] presents the results of several simple test cases designed to expose coding errors or other fundamental errors in the representation of the magnetic force. For example, fields with constant values for ∇H, with and without free surfaces, with different orientations of field and free surface, were simulated to observe the resulting fluid motion. In all cases, as predicted by theory, steady-state pressure contours were coincident with lines of constant field strength, and the free surfaces moved through the field until they also became coincident with surfaces of constant field strength. The surface shapes and flowfields predicted by the computational model were in agreement with the known analytical solutions for all preliminary test cases.

For comparative purposes, the geometry of the tank used in all of the simulations presented was that of the experiment test tank used in the MAPO program. As shown in Fig. 1, the 152-mm-diam cylindrical tank is 248 mm in height and positioned 17.5 mm above the magnet. The magnetic properties of liquid oxygen (LOX) and the fluid properties of water were used to simulate the ferrofluid used in the experiment. The centerline of the MAPO tank is coincident with the axis of a ring magnet with a 101-mm i.d., a 254-mm o.d., and a height of 40 mm. The magnetic field axis is along the ring's geometric axis, and it produces a magnetic field strength of approximately 0.4 T at north face. (North is at the top flat face and south at the bottom face) Hochstein et al.,[14] Warren,[15] and Hochstein[16] modeled the field produced by this magnet with the field solution for a magnetic dipole and used the simulation to make preflight flowfield predictions of the experiment.

The magnetic dipole is a typical far-field approximation and was appropriate for the initial experiment configuration. The dipole strength was specified to match magnetic field strength measurements made along the tank centerline. Results from preliminary experiments motivated a redesign of the apparatus that reduced the size of the tank and changed its shape. In the new configuration, a significant portion of tank's fluid content is so close to the magnet that the far-field assumption no longer seemed reasonable. Therefore, a detailed survey of the field in the region occupied by the tank was made. The new experiment configuration is shown in Fig. 1, and the measured field is depicted by contours of constant H in Fig. 2. For both the dipole and measured models, the magnetization of the liquid was assumed to have negligible influence on the imposed magnetic field.

A 95×163 orthogonal computational mesh used for each simulation. Each rectangle in the mesh represents an annular ring consistent with the cylindrical geometry of the tank. The tank centerline is coincident with the left boundary, and the right boundary represents the tank wall. The mesh has been refined in several locations to resolve particular flow features typically observed in studies of MPP. Mesh refinement along the wall is necessary to resolve the thin layer of fluid that is observed to move along the wall during the reorientation process. Regions near the centerline and tank bottom have been highly refined to avoid numerical difficulties experienced in locations of high magnetic field gradients.[17]

Computational Fidelity

The only data available for code validation directly related to MPP are the preliminary data from the MAPO experiment. The only flowfield data available are for a tank fill level of 50%, and these data are in the form of video recordings and still-frames extracted from those recordings. Although not opaque, the ferrofluid/water mixture attenuates light passage so rapidly that details of the flow internal to the tank surface cannot be seen. Furthermore, the angle of view for the recordings is not normal to the cylinder, and so problems with data interpretation due to the refraction of light as it passes through the cylindrical wall of the acrylic tank are exacerbated. Figure 3 presents a sequence of flowfields recorded for a configuration in which liquid is collected at the magnet end of the tank before it enters the reduced gravity phase of the KC-135 flight. Figure 4 presents a flowfield sequence corresponding to a configuration in which liquid is initially collected in the end of the tank opposite to the magnet. Although the resolution observable in Ref. 8 is a little better, it is still very challenging to discern and evaluate the shape of the liquid free surface as the flow evolves. To simplify further discussion, the magnet end of the tank will be called the bottom of the tank and the end opposite to the magnet will be called the top.

A sequence of flowfields predicted by the computational tool for the 50% bottom fill case are presented in Fig. 5. Vectors for the largest velocities in the bulk motion of the fluid are included in the simulation results. After 1 s, there has already been considerable displacement of the initial flat interface, and a general sweeping motion of fluid from the centerline toward the tank wall can be observed. After 2 s, the interface near the tank centerline appears to have taken on a shape corresponding to a classical meniscus due to surface tension. In contrast, near the tank wall, it appears that momentum imparted by the initial sweep of fluid toward the wall is causing a thin layer of fluid near the wall to climb toward the top of the tank. From this time onward there is little displacement of the free surface in the vicinity of the tank centerline, but a continuing evolution of the thin fluid layer near the wall can be observed. The layer appears to thin and recede.

Figure 6 presents flowfield predictions for the 50% top fill case. It appears that the flowfield predicted at an elapsed time of 1 s is

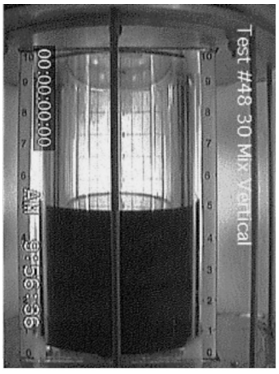

t = 0 sec.

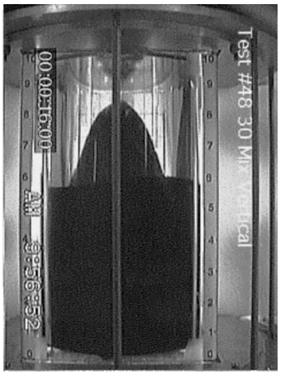

t =16 sec.

t =21 s

Fig. 3 MAPO experiment bottom fill, 50% (time in seconds).

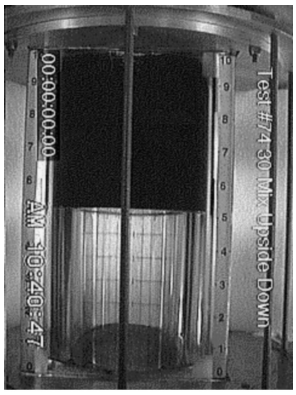

t = 0 sec.

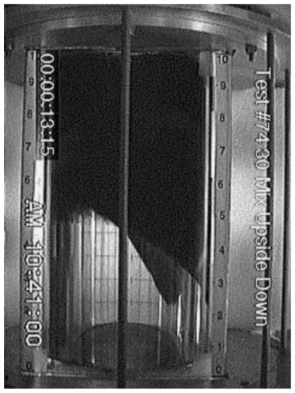

t = 13 sec.

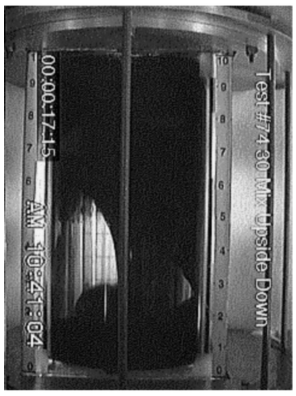

t = 27 sec.

Fig. 4 MAPO experiment top fill, 50% (time in seconds).

the mirror image of that predicted for the 50% bottom fill case at the same point in time. Likewise, the fields predicted for the two cases are nearly mirror images of each other after 2 s of experiment time. Beyond that time it is clear that the magnet is pulling fluid along the wall toward the bottom of the tank. After 30 s, a small pool of liquid has collected at the bottom outside corner of the tank. Note that, although fluid momentum induces flow along the bottom toward the centerline, the magnetic force is strong enough to capture the liquid and hold it in the corner. Although the shape of the free surface of this pool appears to be dominated by surface tension near the tank wall, along the bottom it flattens as the influence of the magnetic field starts to overtake that of surface tension.

Comparison between the computation and experiment is complicated by several factors. Data reduction difficulties associated with optical considerations have already been discussed. In addition to those difficulties, there are important differences between the simulation and experiment that must be addressed. The experiment initial conditions are determined by the aircraft trajectory before entering the reduced gravity phase of the flight. The simulation begins with a flat interface in normal gravity and changes to zero gravity in the first time step. The experiment transitions from a $2g$ environment during the bottom part of the aircraft trajectory to a very low gravity environment during the upper part of the trajectory. The transition takes a finite amount of time and accelerometer data show an elapsed time of 8–10 s before the typical experiment environment has dropped to less than $10^{-3}g$. Beyond that time, the acceleration environment is often uncertain because it drops below the minimum threshold measurable by the experiment instrumentation.

Another problem with the comparison of simulation predictions with data from the MAPO experiment is that the ferrofluid/water mixture provides only a rough approximation of LO_2 behavior. Because the mixture is dilute, the general mechanical properties (such as viscosity) of the fluid are well approximated by those of water. The magnetic behavior is more problematic. It does not exhibit the

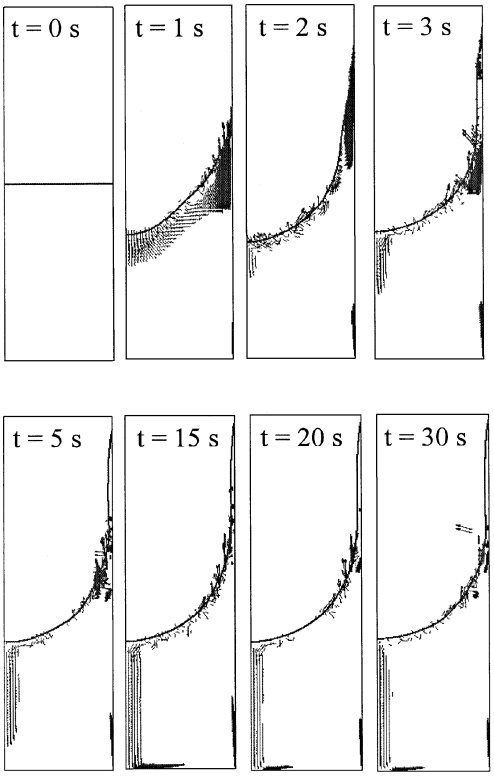

Fig. 5 Bottom fill, 50% (time in seconds).

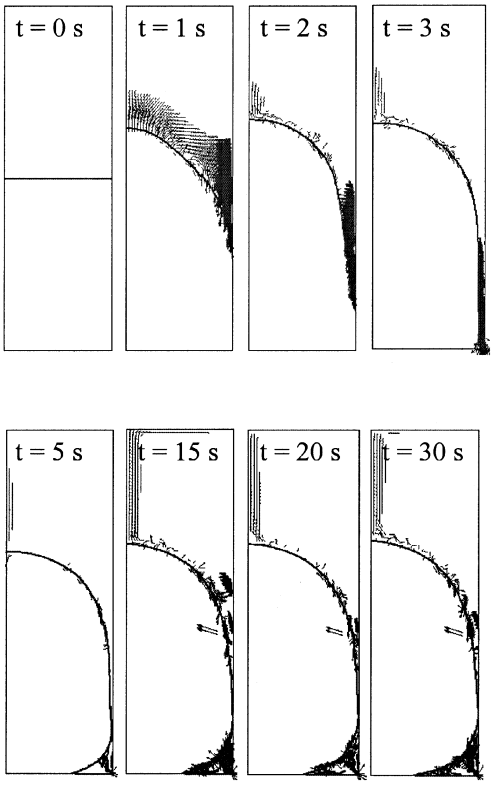

Fig. 6 Top fill, 50% (time in seconds).

linear magnetization expected for LO_2 in a real application and, consequently, is more strongly attracted to the magnet in regions of higher field strength and more weakly attracted in regions of lower field strength.[8]

Although a computational simulation can be defined with symmetric boundary conditions, some measure of asymmetry is almost certainly present in the flight experiment, further complicating comparison of experimental measurements with computational predictions. It has been observed in the computational simulations that the initial fluid interface deformation appears to impart sufficient outward momentum to the fluid to cause a thin layer of fluid to extend along the outer cylindrical wall toward the tank ends. Even a slight misalignment of tank centerline with the initial gravity vector can explain why fluid appears to extend further along the outer wall at some positions than it does at others. The final picture in the bottom fill sequence (Fig. 3) shows that fluid on the far side of the tank has climbed further toward the top than at the near side. The same initial misalignment can explain why the final picture of the top fill sequence (Fig. 4) shows a highly asymmetric interface shape.

Therefore, the challenge is to extract as many meaningful conclusions as possible from a comparison between the experiments and the simulations without looking for an unreasonable level of agreement. Although a 9-s time shift to account for the difference in initial gravitational environments can be assumed, the difference between the abrupt change of the computational simulation acceleration environment and the gradual change of the experiment environment can only be qualitatively considered. The asymmetry of experiment initial conditions was not precisely measured and, even if they were, the present computational tool would be incapable of simulating them. Therefore, conclusions drawn from surface shape comparisons must somehow seek an azimuthally averaged shape for the experimental data. Given all of these caveats, what conclusions can reasonably be drawn? All of the flowfields predicted by the simulations are plausible. Although the video frames show that only a portion of the surface in the bottom fill case appears to have reached the height along the outer wall predicted by the simulation at the end of the experiment, the surface has risen considerably around the entire periphery of the tank. A comparison between experiment and simulation of liquid/vapor interface shape away from the cylindrical wall is prohibited by the opacity of the experiment fluid. In a somewhat serendipitous manner, the asymmetric results of the top fill experiment actually facilitate such a comparison. Although difficult to discern with the small-scale monochrome picture presented in Fig. 4, a larger color picture of the final flowfield of the top fill case does reveal some interesting features. In agreement with the simulation, at the end of the experiment, a noticeable pool of liquid has collected in the bottom corner of the tank. Because flow along the portion of the cylindrical wall closest to the camera has not yet reached the bottom, some details of the interface shape away from the wall can be discerned or inferred. The quantity of fluid observed in the pool is reasonably consistent with the computational prediction. Furthermore, considerable light appears to have been transmitted through the fluid layer on the far wall, allowing a reasonable conclusion that the layer is quite thin as predicted by the simulation.

In summary, there was excellent agreement between the computational tool and analytical solutions for several model problems. In addition to relatively simple test fields filled with fluid, accurate predictions were obtained for surface shapes formed under the influence of magnetic and gravitational forces. Finally, every comparison between MAPO experiment data and simulated flowfield predictions showed as good an agreement as reasonably possible. Therefore, the simulation has been judged suitable for a continuation of the investigation of MPP.

Propellant Reorientation and the Magnetic Bond Number

After the fidelity of simulation for modeling MPP was established, a test matrix was defined to investigate the utility of the magnetic bond number as a predictive tool in the reorientation process. Specifically, simulations were performed to explore the possibility of determining a critical magnetic bond number Bo_m for a range of initial conditions by the use of the MAPO tank geometry and the dipole magnet configuration as shown in Fig. 7. The dipole magnet is expected to be more representative of the type of magnetic field configuration used in a full-scale cryogenic propellant management system and was, therefore, selected for this study. Meaningful evaluation of the reorientation process can only be accomplished by establishment of a uniform quantitative standard.

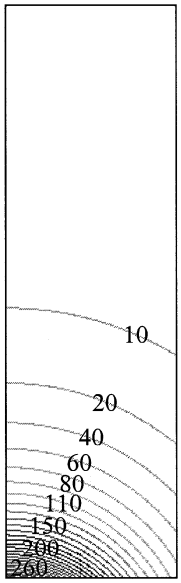

Fig. 7 Contours of constant magnetic intensity, $H(\times 10^3$ A/m), inside the MAPO tank for the dipole model.

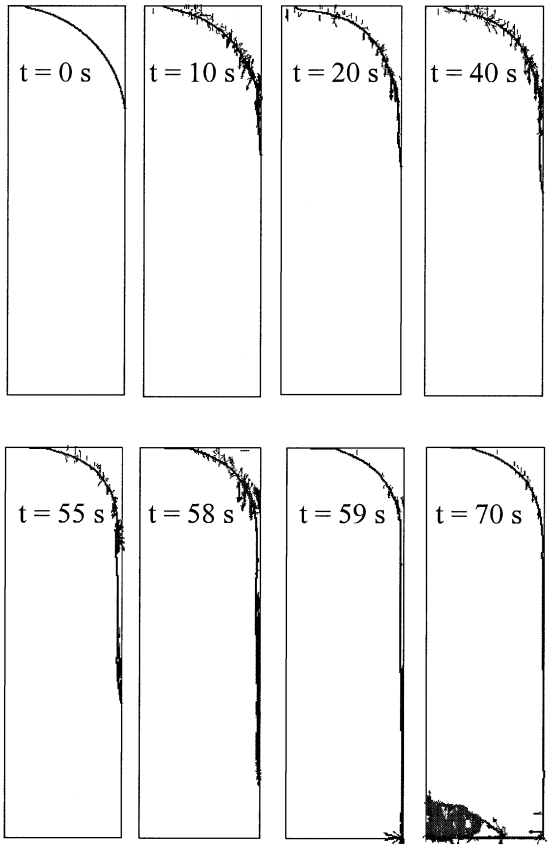

Fig. 8 Paramagnetic propellant reorientation (10% fill/MAPO tank/dipole magnet, $Bo_m = 0.15$).

For this investigation, reorientation is determined by the magnet's ability to influence a reasonable portion of the propellant to traverse the outer tank wall and to come in contact with the opposing tank head. The critical magnetic bond number Bo_m is defined as the value above which reorientation will occur. Because surface tension is constant, differences in the value of the magnetic bond number for a fixed volume reflect changes in the magnetic field strength.

To imitate conditions in a spacecraft tank where reorientation is desired more accurately, the following simulations model the fluid and magnetic properties of LOX and begin with the gas/liquid interface in the shape of a meniscus. Figure 8 presents a sequence of flowfields for a 10% fill and $Bo_m = 0.15$. This example illustrates successful reorientation for the specified magnetic bond number. In this particular case, the gradual ascension of a thin fluid layer along the outer tank wall can be observed through 58 s of simulation time. At 59 s, the fluid has reached the opposing tank head and by definition reorientation is achieved. Beyond 60 s, the formation of a small pool of liquid is observed around the tank centerline and is a consequence of the magnet's location along the centerline. The shape of the free surface of the pool is driven by the magnetic force as it conforms to a surface of constant magnetic field strength.

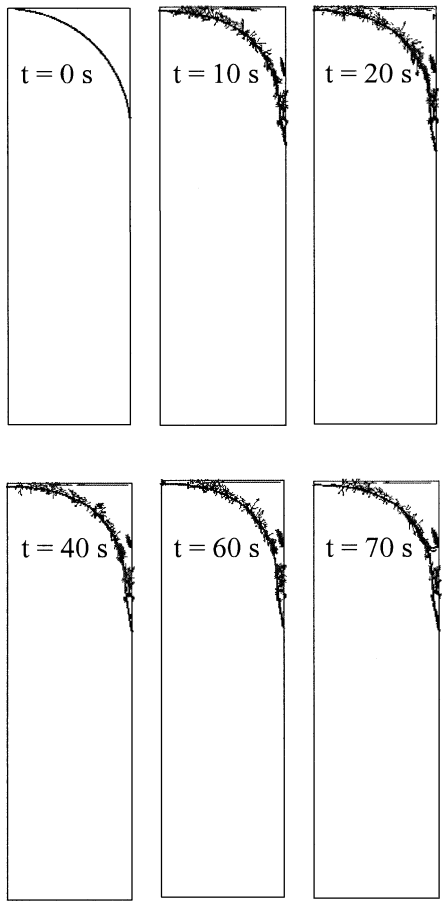

Fig. 9 No reorientation (10% fill/MAPO tank/dipole magnet, $Bo_m = 0.14$).

In contrast, Fig. 9 depicts flowfield predictions for the same 10% fill level simulated at a lower magnetic bond number, $Bo_m = 0.14$, and exemplifies a case in which propellant reorientation does not occur. In this case, only a slight deformation in the shape of the initial free surface is observed through the entire simulation. The final shape of the gas/liquid interface appears to be influenced strongly by surface tension. However, the noticeable extension of the fluid interface near the tank wall suggests that the magnet is attracting this layer toward the bottom, but the attraction is not strong enough to induce reorientation.

For this study, an initial assumption was made for the value of the critical Bo_m. A sequence of simulations followed in which either an increased or decreased value of Bo_m was specified in a search for the minimum value that would produce reorientation. This process was repeated for each case in the test matrix. Figure 10 presents the critical Bo_m evaluated at each fill level for the flat and hemispherical ends of the MAPO experiment tank. From these results, it is apparent that the relationship between tank fill and critical Bo_m is not linear, but exhibits curvilinear behavior. For both tank shapes, the value of the critical Bo_m increases at a greater rate than fill height decreases. To predict intermediate values of threshold Bo_m without the tenuous computational iterations, an approximating function was sought that would fit the data obtained via the simulation. Visual inspection suggested that a quadratic or simple power series curve fit of the data would be sufficiently accurate. However, the errors between the data points and trend lines for these types of curve fits yielded

Table 1 Bo_m correlations for flat and hemispherical head tanks based on hyperbolic curve fit

	Flat head tank				Hemispherical head tank			
% fill	Bo_m	$Bo_{m,c}$	Error^2	% error	Bo_m	$Bo_{m,c}$	Error^2	% error
10	0.15	0.150991	9.83×10^{-7}	0.66092	0.12	0.12118	1.39×10^{-6}	0.98217
20	0.09	0.08545	2.06×10^{-5}	5.04807	0.08	0.0744	3.18×10^{-5}	7.05120
30	0.06	0.059592	1.66×10^{-7}	0.67991	0.05	0.0564	1.32×10^{-5}	7.27169
40	0.04	0.045746	3.30×10^{-5}	14.3657	0.04	0.0419	3.79×10^{-6}	4.86475

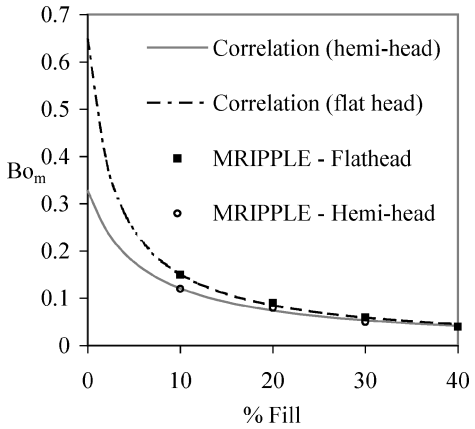

Fig. 10 Bo_m correlation predictions for a hemispherical and flat head tank geometry.

under-predicted values with errors peaking at 30%. Therefore, these fits were concluded to be unacceptable. A hyperbolic fit, amongst all functions considered, proved to minimize the discrepancy between the data and curve. To obtain the appropriate curve fit, a hyperbolic expression relating Bo_m and fill height was defined as

$$Bo_{m,c} = \alpha/[\beta + \gamma(\text{fill fraction})] \tag{8}$$

where α, β, and γ are constant coefficients to be determined. A linear regression technique was employed to evaluate the constant coefficients, and the correlated Bo_m results, $Bo_{m,c}$, for the flat and hemispherical tanks are presented in Table 1. Although the maximum percent error of the flat top tank is approximately 14% for the 40% fill, the error is not detrimental from the point of a design tool because the predicted value is an overprediction of the simulation data point. Furthermore, the Bo_m data points obtained from the simulations are only limited to single-digit precision. In this case, a slight overprediction by the use of the curve fit would still guarantee that the predicted value $Bo_{m,c}$ would induce reorientation. In contrast, an underpredicted value might lie below the true reorientation threshold for a particular fill level, eliminating any guarantee of reorientation and ultimately diminishing the utility of the curve fit for future predictions. The relative percent error associated with $Bo_{m,c}$ for the hemispherical heads peaked at 7% and occurred for the 30% fill level. Again, this proved to be a minor overprediction of the value obtained from the computational simulation and should not devalue the significance of the predicted $Bo_{m,c}$ data. Aside from the two over-predicted data points mentioned, the $Bo_{m,c}$ for the remaining tank fills are an excellent match by the use of the hyperbolic curve fit.

It is interesting to compare the results in Fig. 10 for the hemispherical head and flat head tanks. Whereas the hyperbolic expression provides a good Bo_m fit for the two tanks, the trend lines differ in rates of curvature at lower fill levels, yet the curves appear to converge at greater fill levels. This trend is, in fact, consistent with the nonlinearity of magnetic field strengths for the dipole magnet model. Because magnetic field intensity is inversely proportional to the cube of the distance from the dipole, the magnetic forces acting on the propellant are considerably weaker in the magnet's far field where the gradients are much lower. Therefore, significantly higher magnetic bond numbers are required to reorient propellant for tank fills less than 10% because the majority of the liquid lies within the magnetically weaker far-field region. In a comparison of the two tanks, the differences in Bo_m requirements for reorientation at the lower fill levels can be directly attributed to this magnetic effect. Specifically, the position of the bulk fluid is shifted toward the magnet in a tank with hemispherical heads as compared to the tank with flat heads. This position shift is solely due to the change in geometry, yet it is significant enough to produce a 20% increase in magnetic bond number needed to induce reorientation in the flat head tank as compared to the hemispherical-head tank. This slight shift in the propellant position, gained by the use of a tank with hemispherical heads, forces more of the propellant into regions of higher magnetic field strength, reducing the Bo_m reorientation threshold. In contrast, the shift is less significant for greater tank fills because a substantial portion of the fluid, in either case, is positioned in regions of rapidly changing magnetic field strength, which yield higher magnetic gradients, and, consequently, impart a stronger magnetic force.

Evidence for this magnetic influence can easily be observed in the sample reorientation flowfield predictions presented earlier in Fig. 8. Even after 55 s of the simulation time, the thin fluid layer extended only 50% of distance of the outer wall. Clearly, surface tension is contributing to the slow fluid motion because the magnetic forces are much weaker near the top tank head. However, within 4 s, the fluid layer has traversed the entire outer wall, and approximately one-half of the fluid has already reoriented into a pool near the centerline. The differences in the time required to impart motion through the simulation are explicitly attributable to the nonlinear magnetic influence discussed. As the fluid approaches the magnet, the applied magnetic forces become significantly stronger, reducing the time required to move between locations within the tank.

Note that the portion of the two curves that predicts Bo_m for tank fills less than 10% is an extrapolation of the simulated data. Based on experience, these curves may reasonably predict the reorientation threshold for these lower fill levels; however, data are not currently available to substantiate this conclusion.

The second set of cases was selected to examine the influence of gravity on the magnetic reorientation process. This influence should be observable by comparison of Bo_m reorientation thresholds for zero-gravity and reduced-gravity simulations. This influence should also be reflected in differences between reorientation times for a range of magnetic field strengths (Bo_m) and fill levels. Note that negative values indicate a gravity vector oriented toward the tank head closest to the magnet and positive values in the direction toward the opposing tank head. Figure 11 presents the critical Bo_m for each fill level for zero-g and $-1 \times 10^{-7} g$ simulations. In both cases, the relationship between tank fill and critical Bo_m is curvilinear. The value of Bo_m increases at a greater rate than fill height decreases.

For a tank fill of 10%, the simulation predicts a negligible influence of gravity on the critical Bo_m. At such a small level of gravity, this negligible influence can be attributed to the smaller magnetic field gradients experienced in the magnet's far field. However, differences in threshold values up to 20% are noted at intermediate fill levels. These predicted variations are, in fact, contrary to the preconceived hypothesis that the influence of negative gravity should assist in propellant reorientation and decrease the critical Bo_m at a particular fill level. Intuitively, if gravity and the magnetic field are both contributing a downward force on the fluid, some reduction in reorientation time should be observed compared to a similar simulation without gravity. Two plausible arguments support these unexpected results. First, consideration was given to the influence of gravity on the initial shape of the fluid free surface. Because gravity tends to

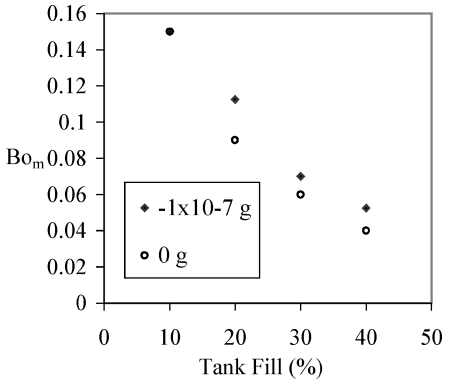

Fig. 11 Critical Bo_m comparison between zero- and reduced-gravity (MAPO tank/dipole magnet/20% tank fill).

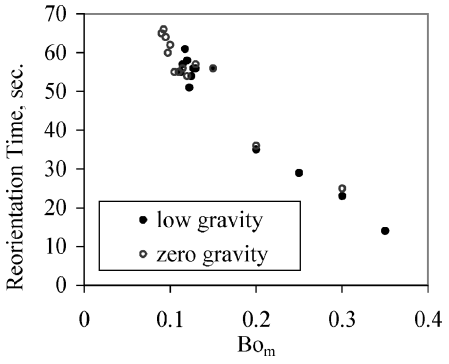

Fig. 12 Reorientation time vs Bo_m for zero- and reduced-gravity (MAPO tank/dipole magnet/20% tank fill).

reduce the curvature of the interface shape, the initial location of the free surface near the outer tank wall may be slightly shifted away from magnet. Similar variations observed in critical Bo_m between the flat head and hemi-head tank support the conclusion that a slight difference in the initial position of the propellant can change the critical magnetic bond number by up to 20%. A second factor was uncovered by extension of the investigation to reorientation timing with respect to magnetic field strength. Figure 12 presents reorientation times for a range of magnetic field strengths in terms of Bo_m in a zero-g and reduced-gravity environment for a fill of 20%. As expected in both cases, reorientation times decrease for larger values of Bo_m. However, erratic reorientation behavior is exposed near the critical Bo_m. The oscillations in reorientation time near the threshold Bo_m are observed in both the reduced-gravity and zero-gravity simulations. A qualitative study of flowfield results does indicate a certain level of jitter in the initial motion of the bulk flow in all simulations. This behavior is quickly dampened at higher levels of magnetic field strength where the magnetic forces are a dominant influence on the bulk fluid motion. Yet, this behavior is noticeably observed at lower values of the Bo_m near the threshold. Because all traditional numerical stability criteria were conservatively satisfied during each simulation, the oscillations are suspected to be a result of the near parity of surface tension and magnetic forces near the critical magnetic bond number. The effects of assisted reduced gravity become noticeable in reorientation times well beyond the threshold because the data do converge toward the hypothesized influence of gravity. For a 20% fill level, a gravity force in the direction of the flow does enable shorter reorientation times, but only past an apparent secondary limit in the magnetic field strength that lies well above the critical Bo_m. Further research will be required to explore this behavior for other levels of gravity.

Further evidence for this trend in reorientation times can be sought by a comparison of data for two different fill levels. Figure 13 presents the comparison between reorientation times for a 20 and 30% tank fill with reduced gravity. The same erratic pattern is observed in reorientation times near the critical Bo_m. A more predictable behavior occurs in both cases well beyond the threshold. As expected, the magnetic field strengths required to reorient the 30% tank fill are lower than those required to reorient the 20% tank fill. Whereas it is difficult to explain the random fluctuations near the threshold, this latter behavior is attributable to the differences in initial position between fill levels with respect to the magnet. For the 30% fill, fluid is initially positioned closer to the regions where the magnetic field strength increases more rapidly. Consequently, these regions of higher magnetic field gradients impart a stronger magnetic force to the fluid.

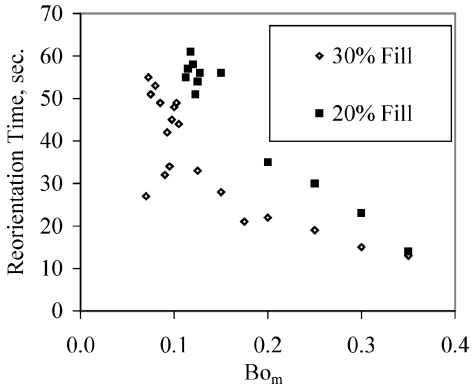

Fig. 13 Reorientation time vs Bo_m for a 20 and 30% tank fill (MAPO tank/dipole magnet/$-1 \times 10^{-7}g$).

Originally, the goal of this investigation and earlier preliminary studies was to determine the minimum Bo_m required to guarantee reorientation under different combinations of initial conditions. The data, however, suggest that predictable flow behavior occurs beyond a certain magnetic field strength that lies above the value of the critical Bo_m. Whereas a more thorough study of dependent variables is required to define this point adequately as a definitive common trend in reorientation timing curves, this limit may prove to be a better definition of a minimum required magnetic field strength for practical application. The critical Bo_m can potentially guarantee reorientation, but the secondary point may guarantee reorientation and signify a lower limit to reliable prediction of reorientation times for any particular set of initial conditions.

Summary

The development of a computational tool designed to complement the experiment program by providing high-fidelity simulation of the MPP process has been presented. A brief description has been presented of the mathematical and numerical models on which the simulation is built. To establish simulation credibility, flowfields from simulations of the MAPO experiment have been compared to data from the experiment, and they were found to be in good agreement.

The ability to model propellant reorientation in a full-scale tank depends greatly on the ability to model the magnetic field strengths needed to induce reorientation. The flowfield predictions presented earlier for the MAPO magnet demonstrate that a liquid pool can be reoriented by imposition of a magnetic field. The extended studies indicated that a threshold may exist for which the fluid will reorient for each fill level and each tank geometry, and that this limit may be quantifiable in terms of a dimensionless parameter. One parameter that relates geometry, surface tension coefficient, and magnetic field strength is the magnetic bond number.

A computational model was used to investigate the utility of the magnetic bond number as a predictive tool for the reorientation process. This paper presented the analytical and computational development of a relationship correlating the magnetic bond number and propellant fill level, based on the flowfield predictions obtained via the simulation. Results for two types of tank configurations were compared, and an analysis was presented that explored the applicability of this relationship in terms of varying constant coefficients for two types of propellant tank geometries. It was shown that a

hyperbolic curve fit provided excellent predictions of critical Bo_m. Predicted values of Bo_m, at most, yielded minimal overpredictions of the reorientation threshold. Because propellant reorientation is the desired outcome, a slight overprediction of the threshold will not reduce the guarantee of reorientation. The curvilinear correlation observed between tank fill and Bo_m can be attributed to the nonlinear variation in magnetic field strengths at different locations within the tank. In addition, differences in tank shape can significantly effect the critical Bo_m for small tank fills where propellant is initially collected in the magnet's farfield.

The simulation was also used to investigate the predictability of magnetic propellant reorientation under the influence of reduced gravity. Results include comparisons illustrating the influence of reduced-gravity, as opposed zero-gravity, conditions derived with the same tank, fill level, and magnetic field configuration. Data are also presented that illustrate the relationship between the magnetic field strength, represented by Bo_m, and reorientation time for two different fill levels.

The comparison of critical Bo_m predictions under zero-gravity and assisted-gravity conditions yielded results that contradicted expectations. It was shown that stronger magnetic strengths were required for the assisted-gravity simulations at the critical Bo_m. However, a detailed analysis of reorientation timing later revealed evidence of unpredictable reorientation times near the critical Bo_m. A secondary point beyond the critical Bo_m was identified where the presence of negative gravity increased reorientation times as initially expected. This evolution of reorientation curves from random behavior near the threshold to predictable behavior at stronger magnetic field strengths was again observed when results for two different fill levels were compared.

Although the results obtained appear to suggest that cryogenic manipulation by the use of magnetic positive positioning is within the bounds of reasonable prediction, considerable work remains before the robustness of this method can be established. More data are required to obtain a more complete picture of reorientation times and to allow for wider variations in tank shapes, sizes, magnetic field configurations, gravity fields, and fill levels. It would be valuable to determine whether a predictability limit exists beyond the critical Bo_m and if this is a common behavior for the reorientation process. If so, it may be possible to establish a set of curves that identify minimum magnetic field strengths necessary to both guarantee and predict reorientation.

Before ambitious ideas for future space missions can be drawn closer to fruition, the new technologies that will be required to support these endeavors must be developed. Long-duration missions will require an efficient method to position and manage cryogenic propellants onboard spacecraft. This preliminary study lends continued support to the proposition that an alternative technology in reliable propellant management may emerge via the process of MPP.

References

[1]Sumner, I. E., "Liquid Propellant Reorientation in a Low Gravity Environment," NASA TM-78969, 1978.

[2]Aydelott, J. C., "Axial Jet Mixing of Ethanol in Cylindrical Containers During Weightlessness," NASA TP-1487, 1982.

[3]Hochstein, J. I., Patag, A. E., and Chato, D. J., "Modeling of Impulsive Propellant Reorientation," *Journal of Propulsion and Power*, Vol. 7, No. 6, 1991, pp. 938–945.

[4]Schmidt, G. R., Chung, T. J., and Nadarajah, A., "Thermocapillary Flow with Evaporation and Condensation at Low Gravity. Part 1. Non-deforming Surface," *Journal of Fluid Mechanics*, Vol. 295, 1995, pp. 323–347.

[5]Schmidt, G. R., Chung, T. J., and Nadarajah, A., "Thermocapillary Flow with Evaporation and Condensation at Low Gravity. Part 2. Deformable Surface," *Journal of Fluid Mechanics*, Vol. 295, 1995, pp. 349–366.

[6]Hochstein, J. I., and Chato, D. J., "Pulsed Thrust Propellant Reorientation: Concept and Modeling," *Journal of Propulsion and Power*, Vol. 8, No. 4, 1992, pp. 770–777.

[7]Chipchak, D., "Development of Expulsion and Orientation Systems for Advanced Liquid Rocket Propulsion Systems," U.S. Air Force Tech. Rept. RTD-TDR-63-1048, Contract AF04 (611)-8200, July 1963.

[8]Martin, J. J., and Holt, J. B., "Magnetically Actuated Propellant Orientation Experiment, Controlling Fluid Motion with Magnetic Fields in a Low-Gravity Environment," NASA TM-210129, 2000.

[9]Neuringer, J. L., and Rosensweig, R. E., "Ferrohydrodynamics," *Physics of Fluids*, Vol. 7, No. 12, 1964, p. 1927.

[10]Kothe, D. B., Mjolsness, R. C., and Torrey, M. D., "RIPPLE: A Computer Program for Incompressible Flows with Free Surfaces," LANL Rept. LA-12007-MS, Los Alamos National Lab., Los Alamos, NM, April 1991.

[11]Brackbill, J. U., Kothe, D. B., and Zemach, C., "A Continuum Method for Modeling Surface Tension," *Journal of Computational Physics*, Vol. 100, No. 2, 1992, pp. 335–353.

[12]Wendl, M. C., Hochstein, J. I., and Sasmal, G. P., "Modeling Jet-Induced Geyser Formation in a Reduced Gravity Environment," AIAA Paper 91-0803, Jan. 1991.

[13]Sasmal, G. P., and Hochstein, J. I., "Marangoni Convection with a Curved and Deforming Free Surface in a Cavity," *Journal of Fluids Engineering*, Vol. 116, No. 3, 1994, pp. 577–582.

[14]Hochstein, J. I., Warren, R. T., and Schmidt, G. R., "Magnetically Actuated Propellant Orientation (MAPO) Experiment: Pre-Flight Flow Field Predictions," AIAA Paper 97-0570, Jan. 1997.

[15]Warren, R. T., "A Computational Model for Magnetically Actuated Propellant Orientation," M.S. Thesis, Dept. of Mechanical Engineering, Univ. of Memphis, Memphis, TN, May 1998.

[16]Hochstein, J. I., "Computational Modeling of Magnetically Actuated Propellant Orientation," Paper 12, NASA/ASEE Summer Faculty Fellowship Research Reports, NASA Contractor Rept. 205205, Oct. 1996.

[17]Palmiter, R. P., "Numerical Vorticity Due to a Strongly Nonlinear Body Force Staggered Grid Representation," *Proceedings of the AIAA Southeastern Regional Student Conference*, April 1999.